# STUDIES ON THE INTENSE POSITRON SOURCE

**Vadym DENYSENKO**, Taras Shevchenko National University of Kyiv, Ukraine
Supervisor: **Dr. Hayg GULER** (**Dr. Iryna CHAIKOVSKA** and **Dr. Robert CHEHAB**),
Laboratoire de l'Accélérateur Linéaire, IN2P3-CNRS, France

**2016**

## Abstract:

In e-e+ colliders, positron source is a very important part. In this report I will describe the work on the simulations of the different positron sources by using specialized software. The goal of this internship was to create a simulation to compare different methods of producing positrons.

# TABLE OF CONTENTS

# 1 Conventional source

The first step of my work is creating a simple geometry model of the positron production.

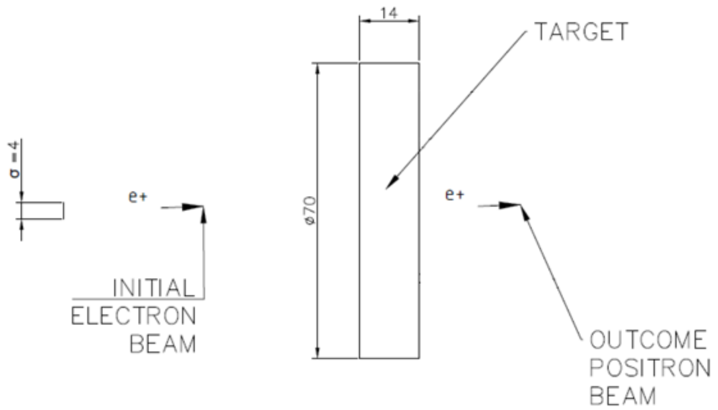


Fig. 1.1 – Schematic representation of task

Beam:

- Type of particles - electrons;
- Shape - circle;
- $\sigma x$ = 4 mm, $\sigma y$ = 4 mm;
- Type of beam - Gauss;
- Energy - 6 GeV;

Target:

- Shape - cylinder;
- Radius - 35 mm;
- Thickness - 14 mm;
- Material - tungsten;

But, before running the simulation we need to setup physics model and some other principal parameters to obtain reliable results.

## 1.1 Range Cuts

To avoid infrared divergence, some electromagnetic processes require a threshold below which no secondary will be generated. Because of this requirement, gammas, electrons and positrons require production thresholds which the user should define. This threshold should be defined as a distance, or range cut-off, which is internally converted to an energy for individual materials. The range threshold should be defined in the initialization phase using the $SetCuts$() method of $G4VUserPhysicsList$.

The idea of a "unique cut value in range" is one of the important features of Geant4 and is used to handle cut values in a coherent manner. For most applications, users need to determine only one cut value in range, and apply this value to gammas, electrons and positrons alike.

In such a case, the $SetCutsWithDefault()$ method may be used. It is provided by the $G4VUserPhysicsList$ base class, which has a $defaultCutValue$ member as the default range cut-off value. $SetCutsWithDefault()$ uses this value.

It is possible to set different range cut values for gammas, electrons and positrons, and also to set different range cut values for each geometrical region.

The $defaultCutValue$ is set to $1.0mm$ by default.

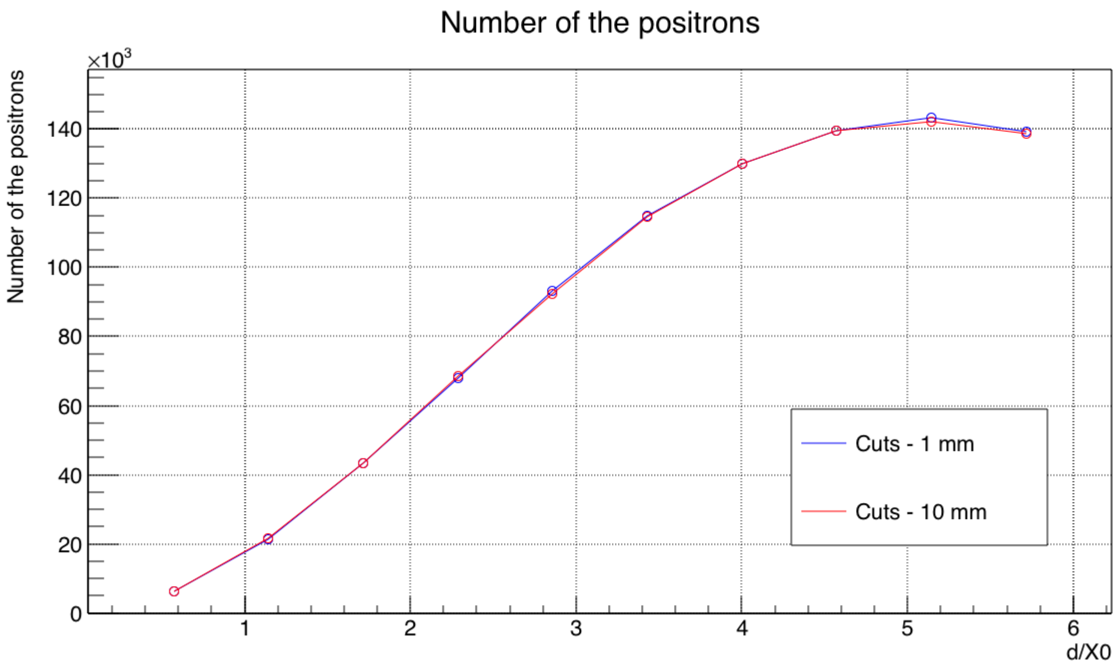


Fig. 1.1.1 – Number of the e+ in dependence of target thickness

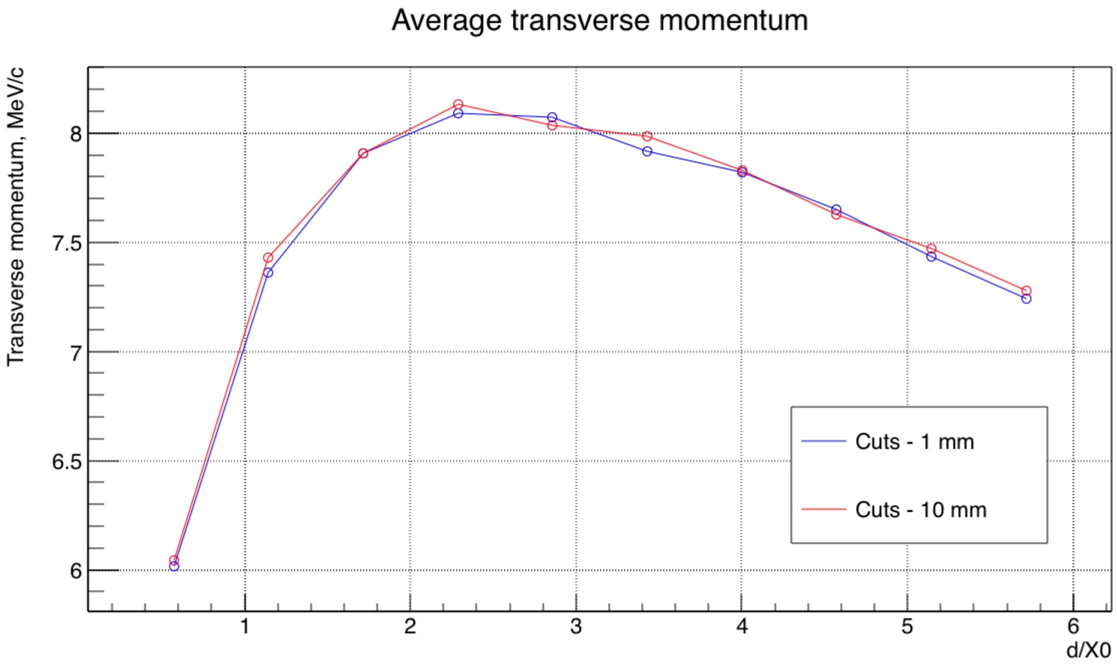


Fig. 1.1.2 – Transverse momentum of the e+ in dependence of target thickness

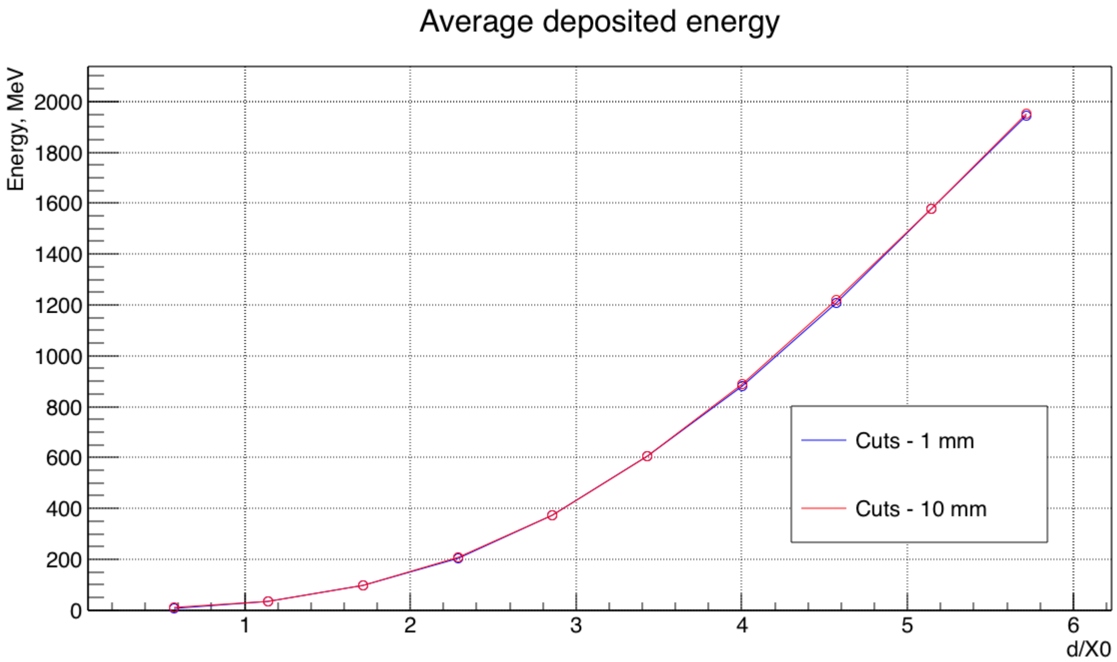


Fig. 1.1.3 – Average deposited energy of the e+ in dependence of target thickness

How we can see, we have no such big difference between a result of the simulations with range cuts value 1 mm and 10 mm. That’s why we have no problem to choose what value we need to use. For future simulations, we have decided use 1 mm range cuts value.

## 1.2 Physics List

The next question that we must answer is which physics lists or which physical models we need to use? From the set of Physics lists that has Geant4, we had chosen two main, which we can use and which we will compare. From the set of Physics lists that has Geant4 we had chosen two main, which we can use and which we will compare. This is $QBBC$ and $G4EmStandardPhysics\_option4$ Physics Lists.

### $G4EmStandardPhysics\_option4$

Few words about physical process[1] for positrons, electrons and photons.

***Positrons***

Physics list include such physical processes for positrons:

- Multiple Scattering with some models:
  - Goudsmit-Saunderson Msc Model (high energy limit - 100 MeV);
  - Wentzel VI Model (low energy limit - 100 MeV);
- Coulomb Scattering (with low energy limit - 100 MeV);
- Ionization - Moller-Bhabha Model;
- Bremsstrahlung with:
  - Seltzer-Berger Model (below 1 GeV);
  - Bremsstrahlung Rel Model (low energy limit - 1 GeV);
- Annihilation;

***Electrons***

For electrons we have all of positrons physical processes except annihilation.

[1]Physics Reference Manual (geant4 10.2, 4 December 2015)

***Photons***

- Photo-Electric Effect with Livermore PhE Model;
- Compton Scattering (Klein-Nishina Model) with Low EP Compton Model (high energy limit - 20 MeV);
- Gamma Conversion with Penelope Gamma Conversion Model;
- Rayleigh Scattering;

## $QBBC$

$QBBC$ is used for hadrons and processes associated with them. But it also includes the basics of electromagnetic interaction. Of all physical processes represented in $QBBC$ we are most interested in $G4EmStandardPhysics$ and $G4EmExtraPhysics$ which included in. In general, we can say that we use just $G4EmStandardPhysics$ with $G4EmExtraPhysics$.

***Positrons***

Physics list include such physical processes for positrons:

- Multiple Scattering with some models:
  - Urban Msc Model (high energy limit - 100 MeV);
  - Wentzel VI Model (low energy limit - 100 MeV);
- Coulomb Scattering (with low energy limit - 100 MeV);
- Ionization;
- Bremsstrahlung;
- Annihilation;

***Electrons***

For electrons we have all of positrons physical processes except annihilation.

***Photons***

- Photo-Electric Effect;
- Compton Scattering;

- Gamma Conversion;

$G4EmExtraPhysics$ used only for add synchrotron radiation for positrons and electrons.

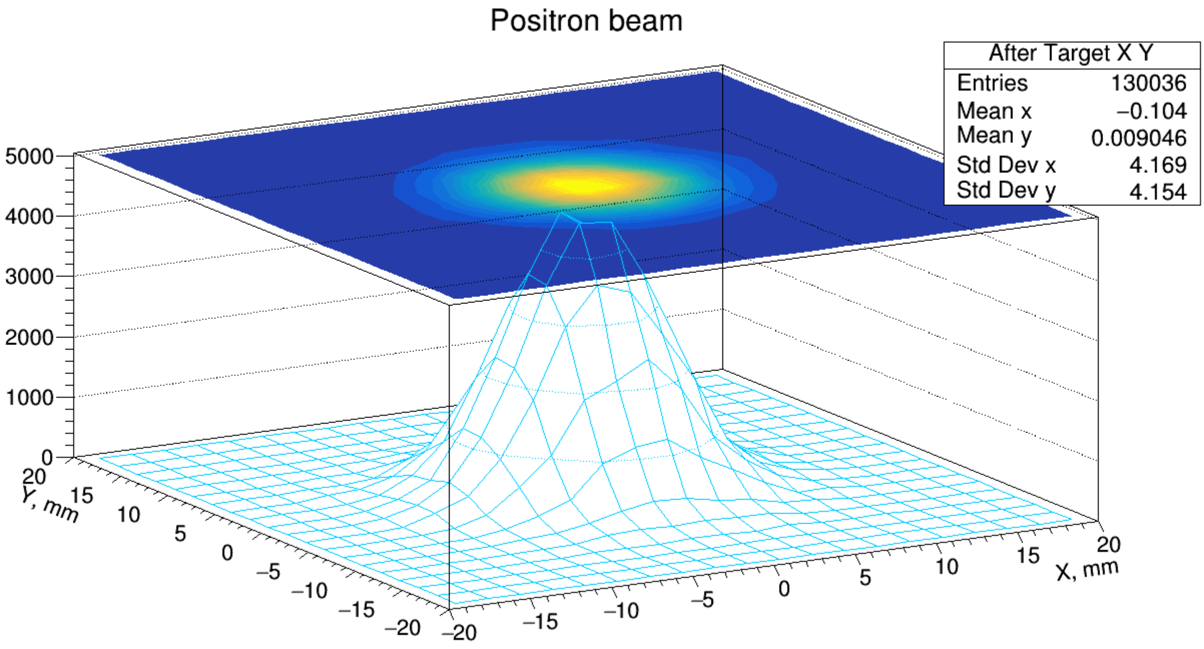


Fig. 1.2.1 – e+ beam after target ($G4EmStandardPhysics\_option4$)

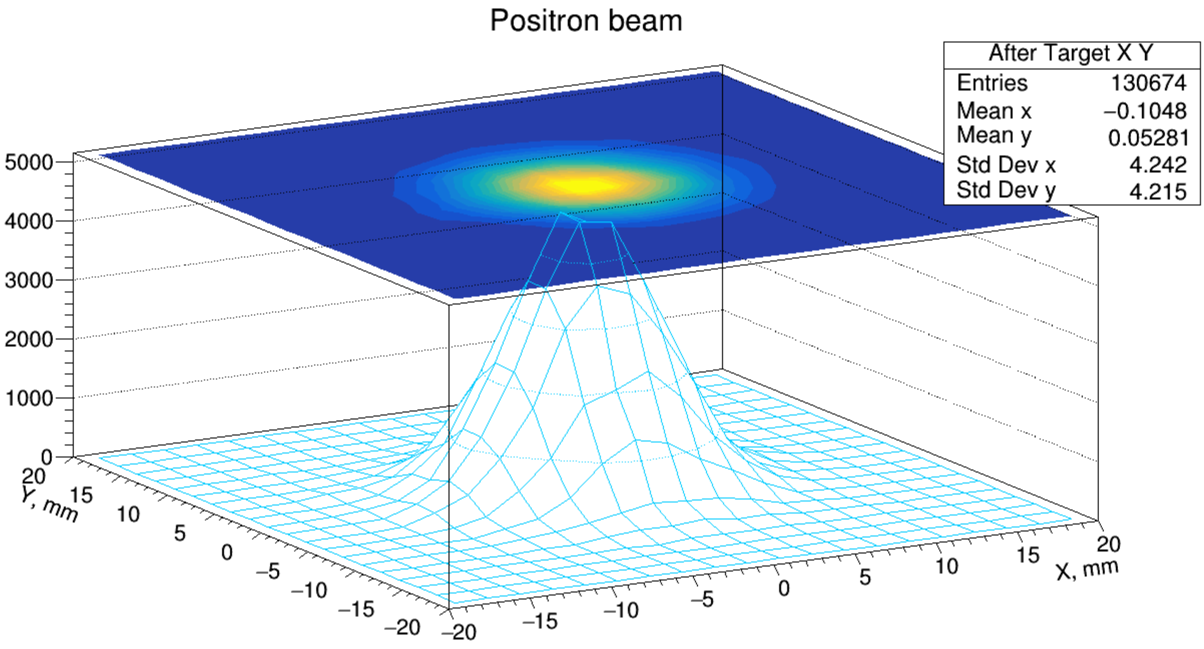


Fig. 1.2.2 – e+ beam after target ($QBBC$)

According to results of the comparison, we choose the $QBBC$ as the main Physics List for our future simulations.

## 1.3 Magnetic field (AMD)

One of the main parts of the positron source is the AMD which include after target for reducing the transverse momentum of the outcome positron beam. That's mean that the schematic representation of task will undergo changes.

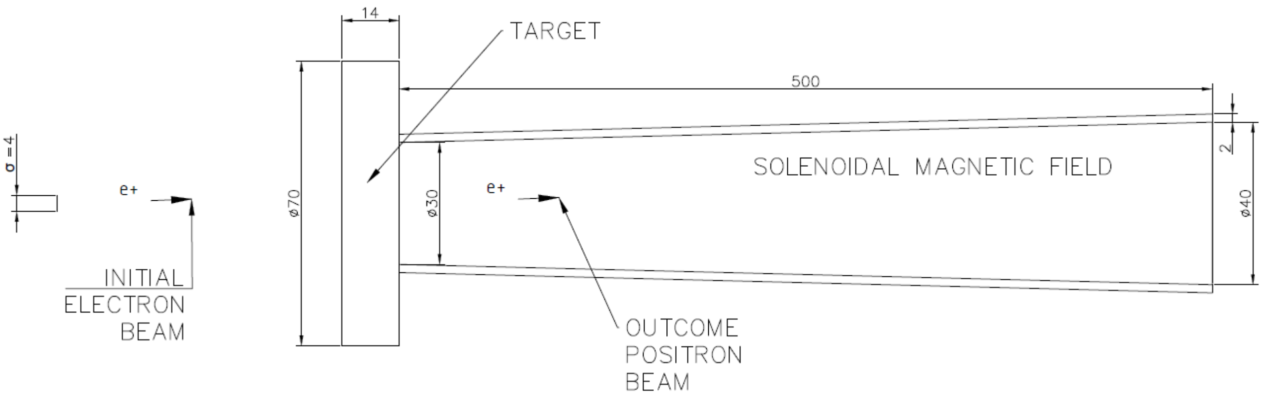


Fig. 1.3.1 – Modern schematic representation of task

Beam:

- Type of particles - electrons;
- Shape - circle;
- $\sigma x$ = 4 mm, $\sigma y$ = 4 mm;
- Type of beam - Gauss;
- Energy - 6 GeV;

Target:

- Shape - cylinder;
- Radius - 35 mm;
- Thickness - 14 mm;
- Material - tungsten;

Magnet:

- Skin:
  - Shape – hollow truncated cone;
  - Thickness – 2 mm;
  - Length – 500 mm;
  - Material – copper;
- Volume with field:
  - Shape – truncated cone;
  - Radius – 15 mm, 20 mm;
  - Length – 500 mm;
  - Material – vacuum.

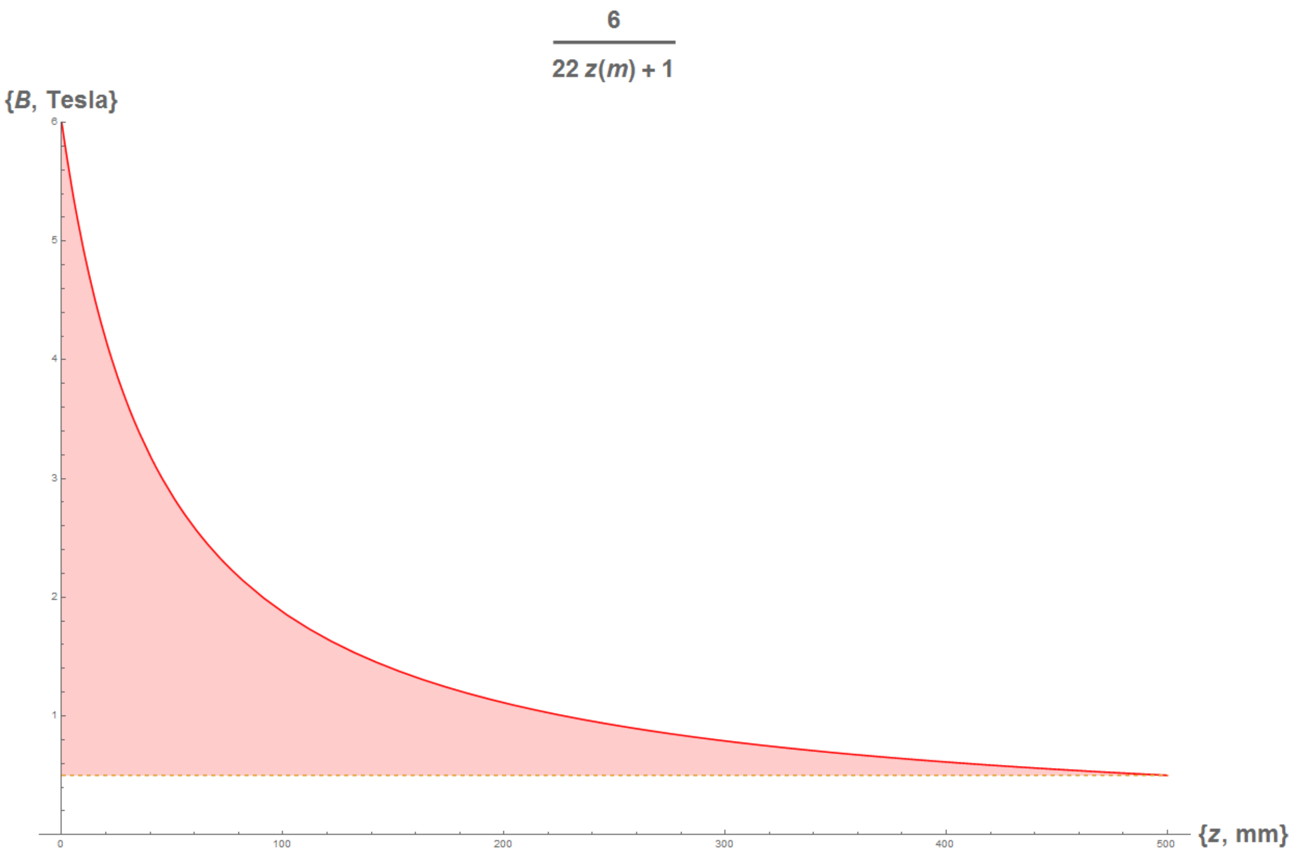


Fig. 1.3.2 – Magnetic field profile

## Some results of the simulation

$N_{e-}^{Initial}$ is number of electrons in initial beam, $N_{e+}^{T}$ is number of produced positrons, $N_{e-}^{T}$ is secondary electrons number and $N_{\gamma}^{T}$ is number of photons after target. $N_{e+}^{M}$ is number of produced positrons, $N_{e-}^{M}$ is secondary electrons number and $N_{\gamma}^{M}$ is number of photons after AMD. $N_{e+}^{bs}$ is number of backscattered positrons, $N_{e-}^{bs}$ is backscattered electrons number and $N_{\gamma}^{bs}$ is number of backscattered photons.

$N_{e-}^{Initial} = 10^5$

$N_{e+}^{T} = 1.285670\ 10^6$, $N_{e+}^{M} = 3.81871\ 10^5$, $N_{e+}^{bs} = 1.4391\ 10^4$

$N_{e-}^{T} = 1.619630\ 10^6$, $N_{e-}^{M} = 5.73677\ 10^5$, $N_{e-}^{bs} = 3.8739\ 10^4$

$N_{\gamma}^{T} = 2.207437\ 10^7$, $N_{\gamma}^{M} = 4.31398\ 10^6$, $N_{\gamma}^{bs} = 1.1773\ 10^6$

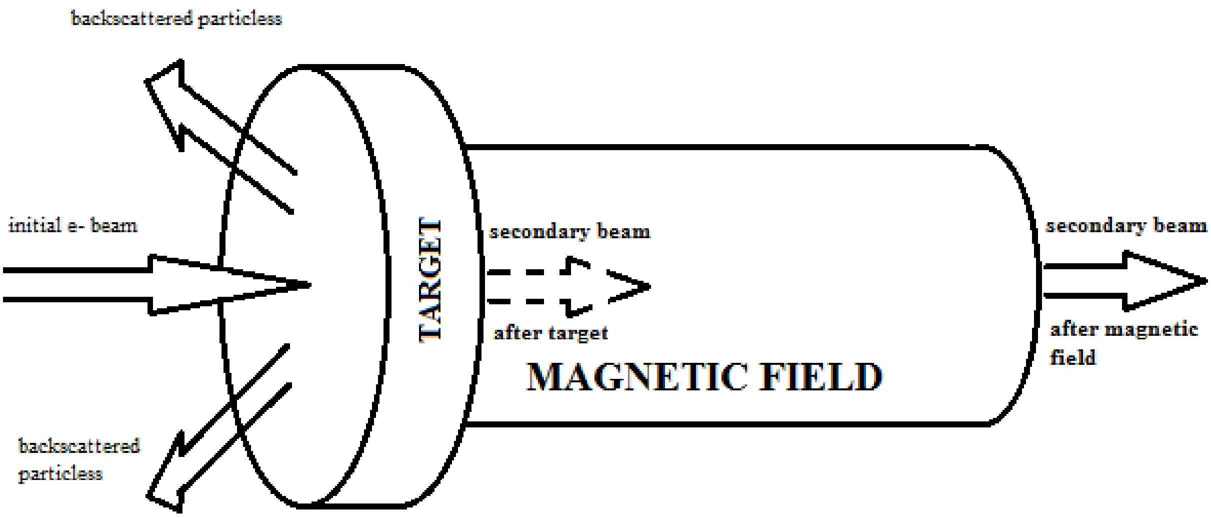


Fig. 1.3.3 – Schematic representation of explored beams

Average number of the generated positrons after target per initial electron is 12.9.

Average number of the positrons after AMD per initial electron is 3.8.

That's mean that after AMD we have about 29% of the generated positrons.

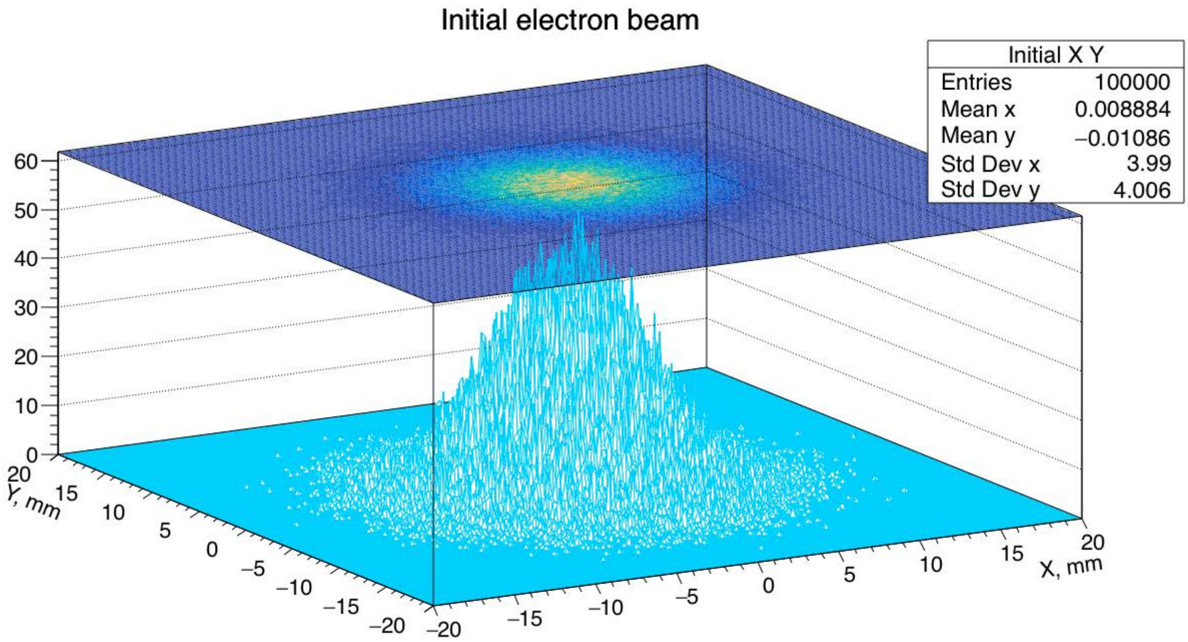


Fig. 1.3.4 – Spatial distribution of the initial $e-$ beam

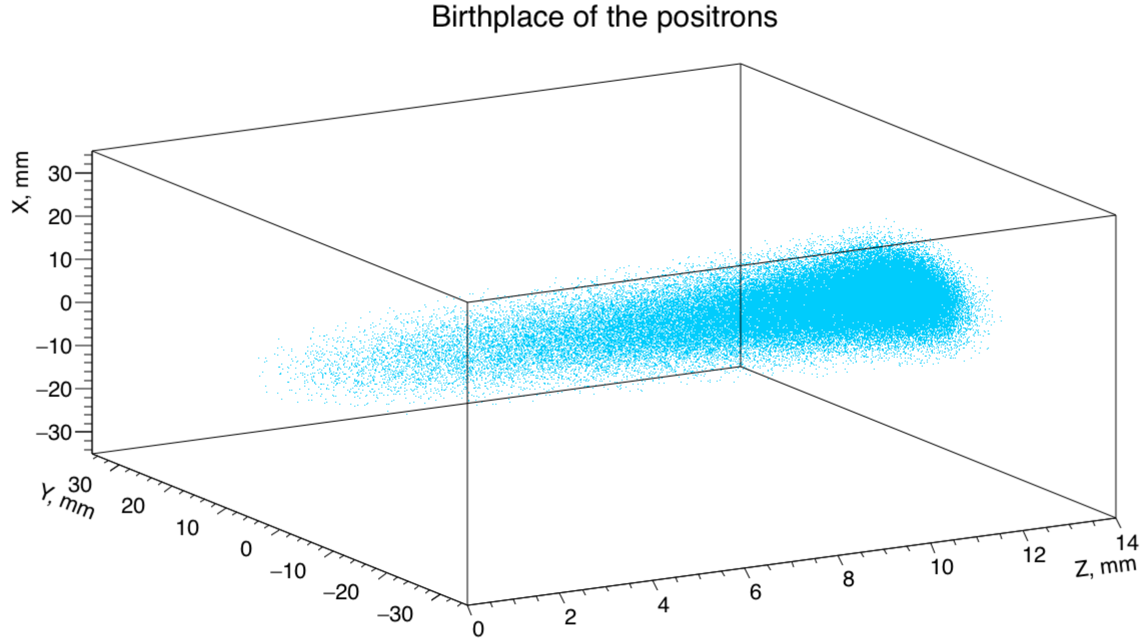


Fig. 1.3.5 – Birthplace of the positrons in the target volume

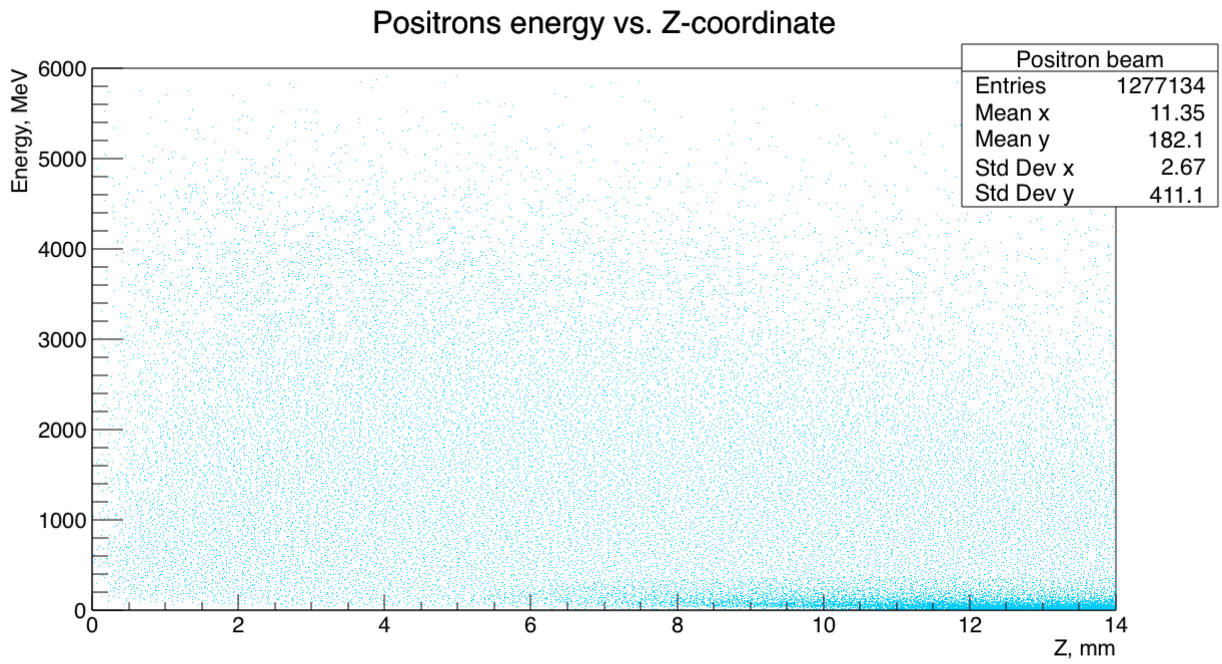


Fig. 1.3.6 – Energy of the produced e+ dependence on Z coordinate of the birthplace

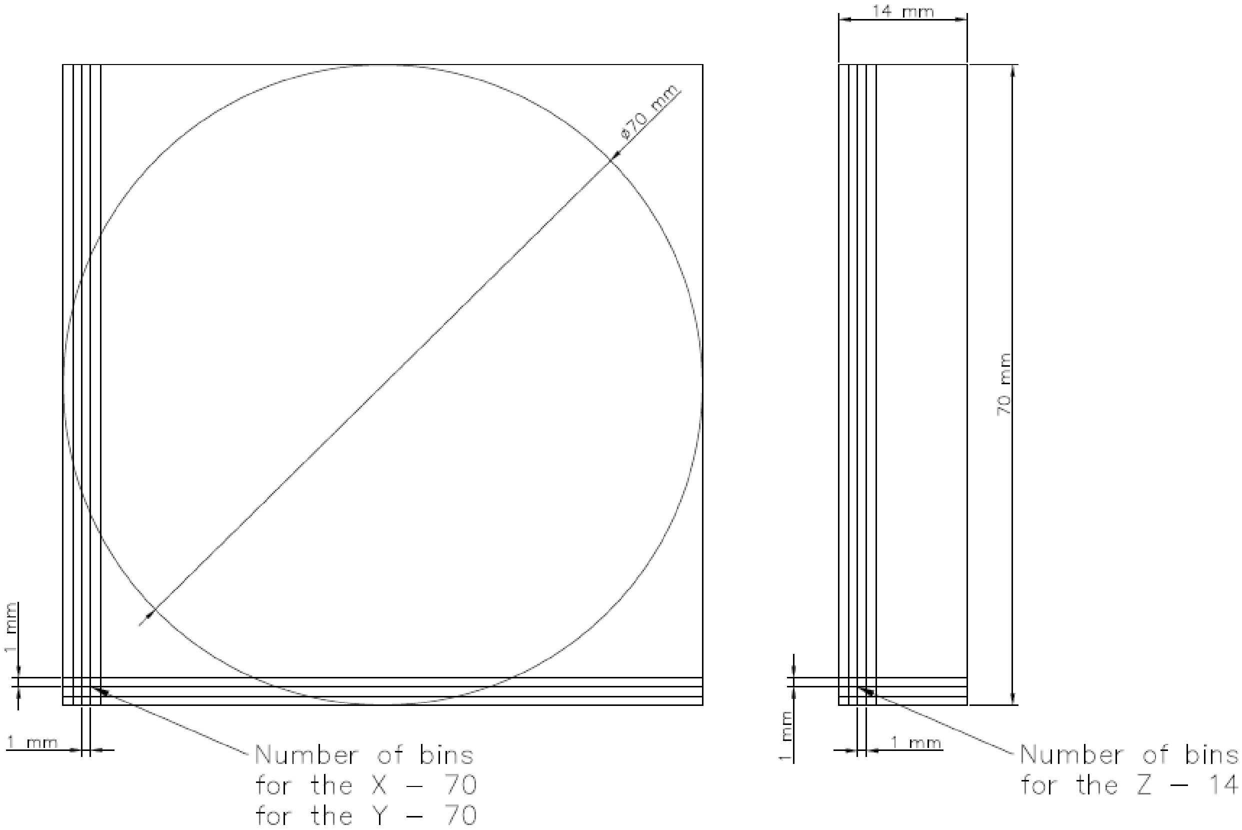


Fig. 1.3.7 – Schematic representation of the target “binning”

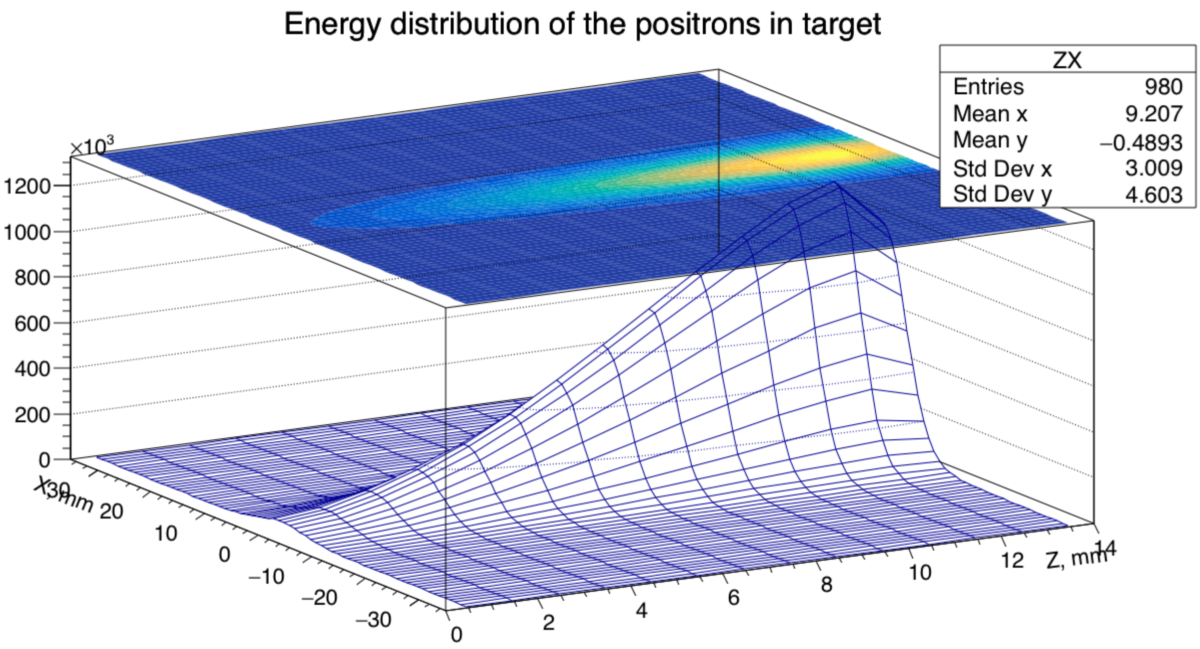


Fig. 1.3.8 – XZ projection of deposited energy distribution in target
(Fig. 1.3.7 binning was used)

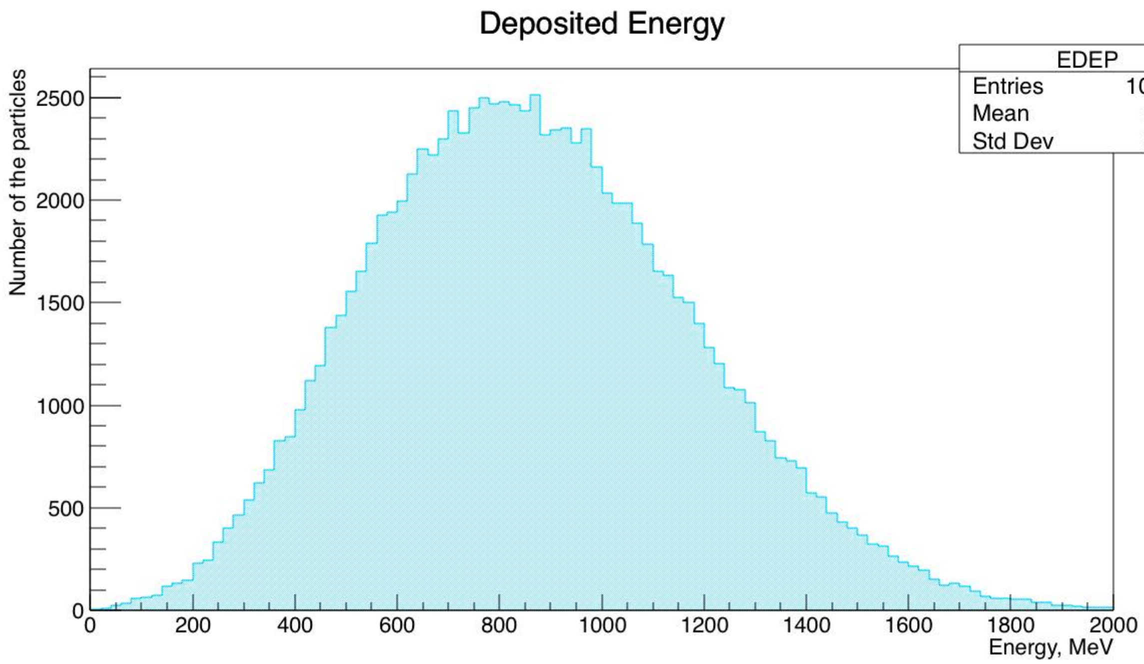


Fig. 1.3.9 – Deposited energy in target

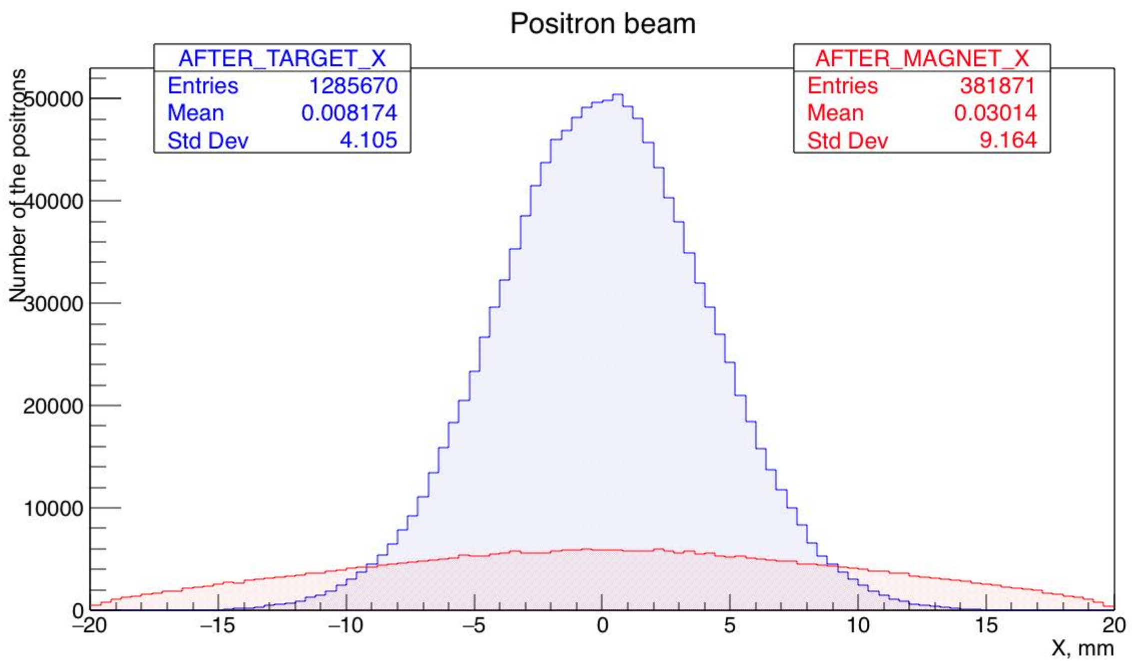


Fig. 1.3.10 - X projection of spatial distribution of the *e*+ beam after target (Blue) and after magnet (Red)

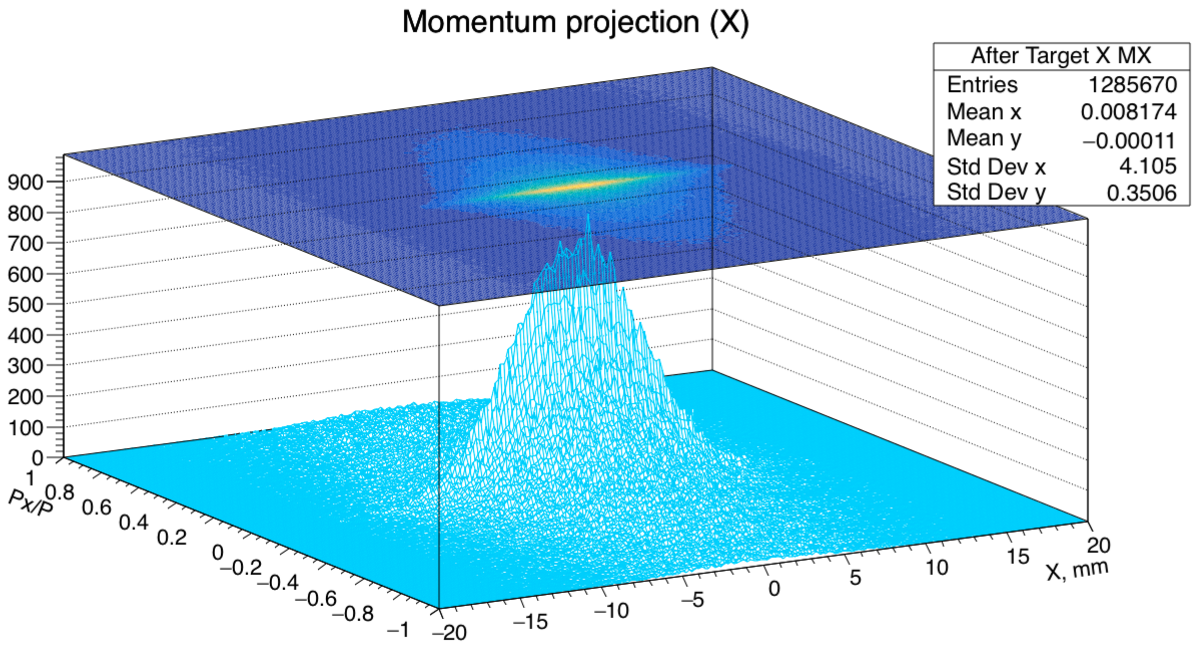


Fig. 1.3.11 – Px/P versus X coordinate of the e+ (after target)

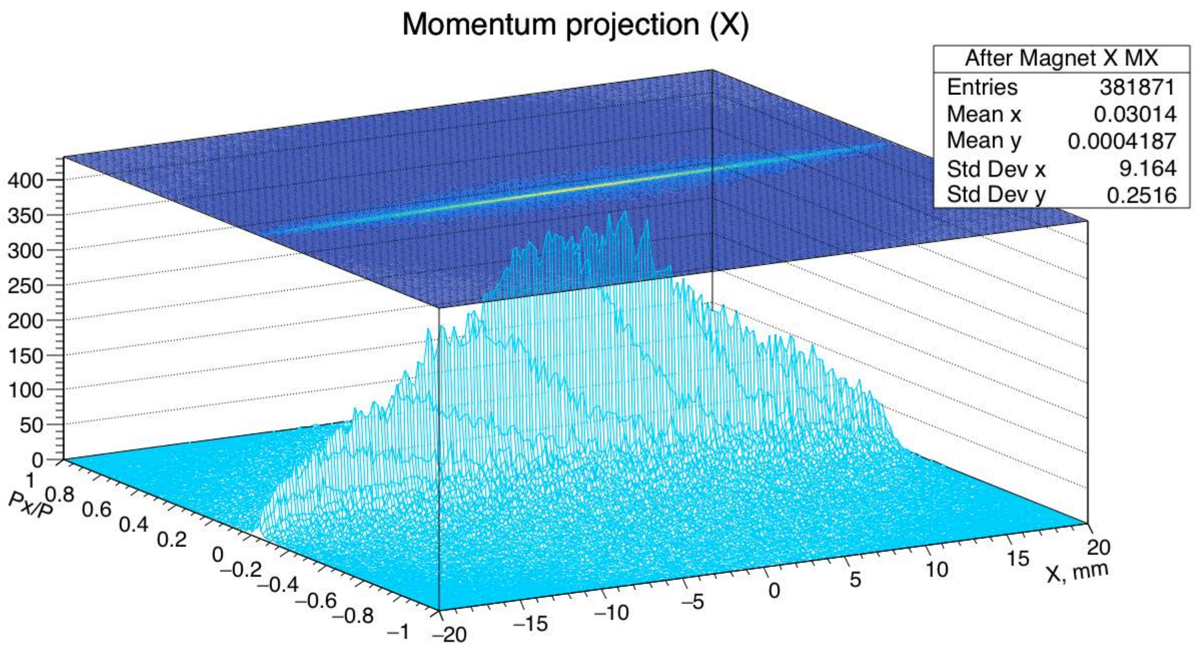


Fig. 1.3.12 – Px/P versus X coordinate of the e+ (after magnet)

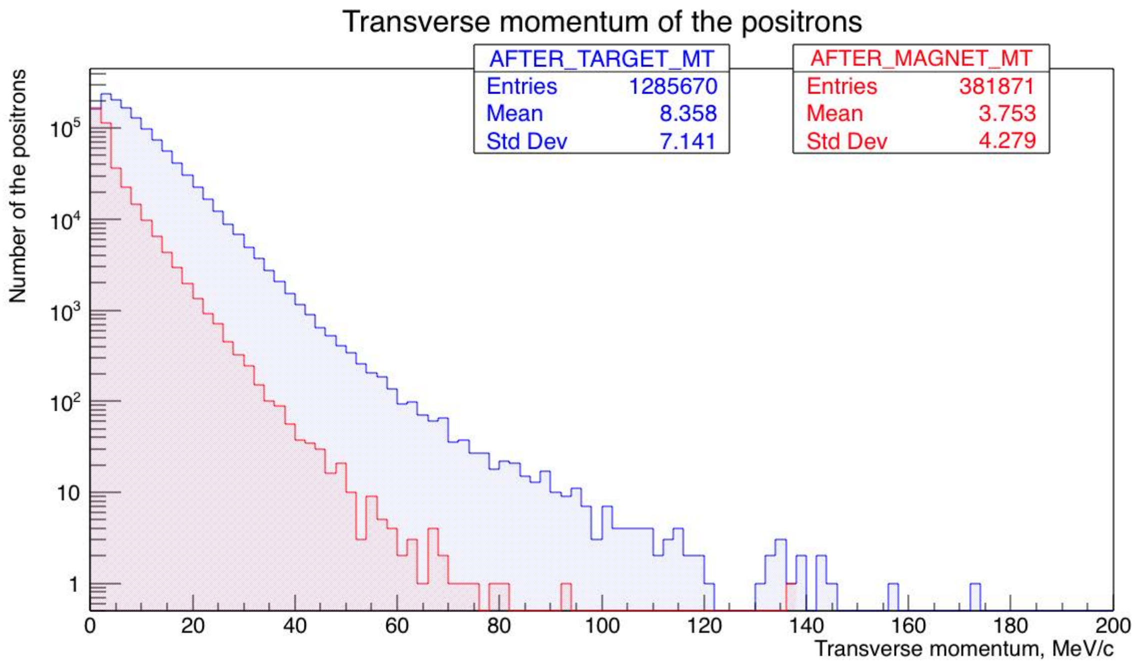


Fig. 1.3.13 – Transverse momentum of the *e*+ (logarithmic scale, after target (Blue) and after magnet (Red))

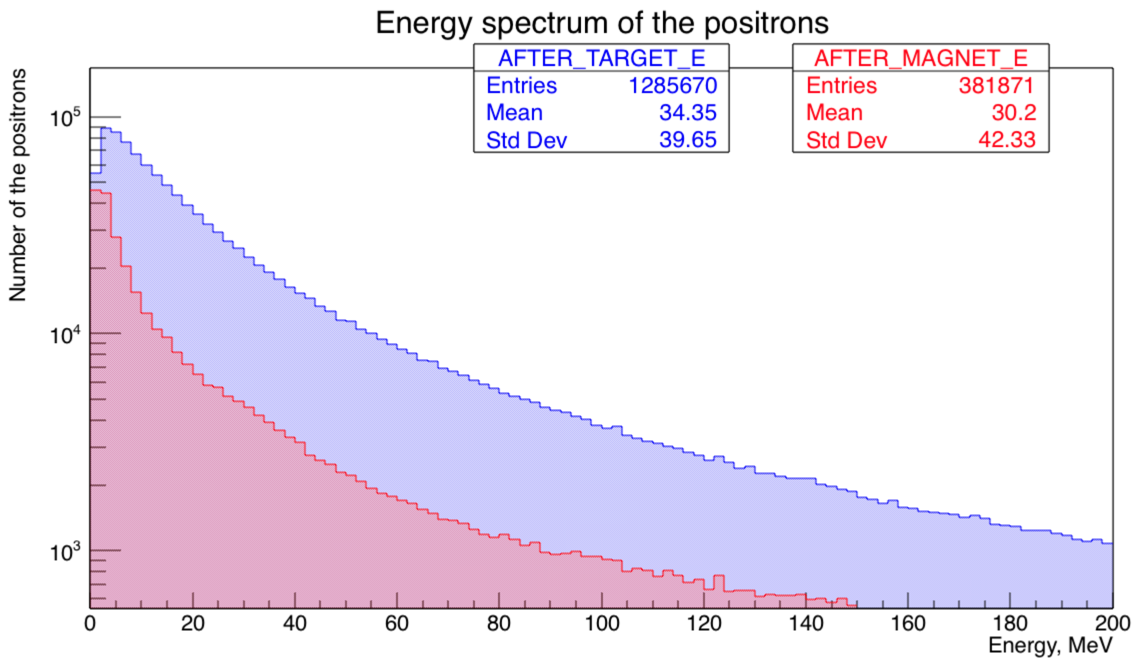


Fig. 1.3.14 – Energy spectrum of the *e*+ (logarithmic scale, after target (Blue) and after magnet (Red))[0 - 200 MeV]

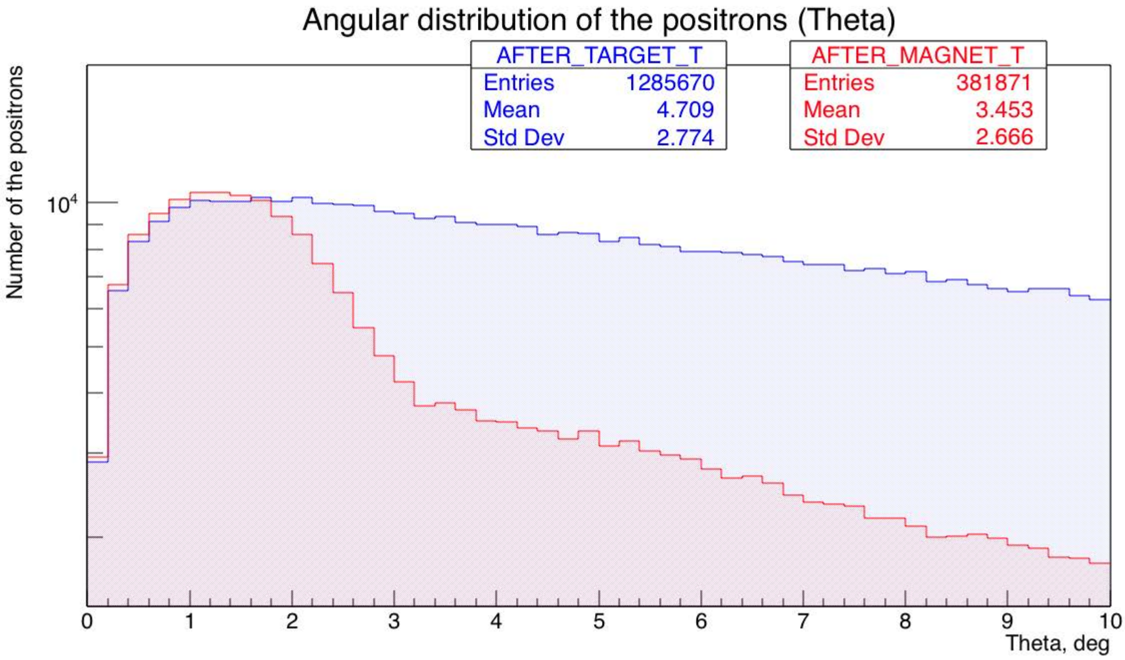


Fig. 1.3.15 – Angular distribution of the $e+$ in dependence of $\theta$ (after target (Blue) and after magnet (Red))[0 - 10 deg]

# 2 Hybrid source

In intense positron source, energy deposition in the target is one of the major problems. To reduce deposited energy, be used so-called hybrid source scheme.

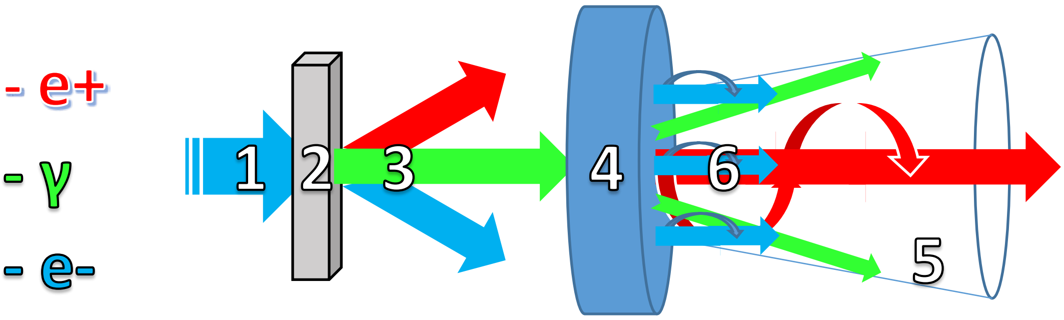


1. Initial e- beam;
2. Crystal;
3. Initial γ beam;
4. Target;
5. AMD;
6. Outcome e+ beam.

Fig. 2.1 – Principal scheme of the hybrid source simulation

The main idea is to use a crystal to producing initial γ beam which hits the target and positrons will be produced.

All work according to this scheme can be separated into two parts. The first one is the production of the photon beam. The second part is the positron production part by using photon beam which has been already generated.

## 2.1 FOTPP

FOTPP is a Monte-Carlo simulation code written by X. Artru using the Baier-Katkov formula for synchrotron radiation in a non-uniform field.

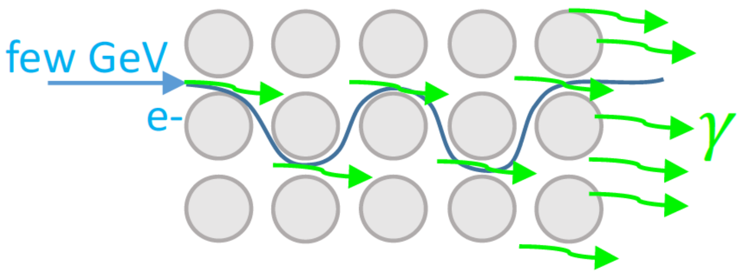


Fig. 2.1.1 - Schematic representation of synchrotron radiation generation

After studying the basic principles of FOTPP I had to compare the results of simulation of this program and program which was written by V. Strakhovenko.

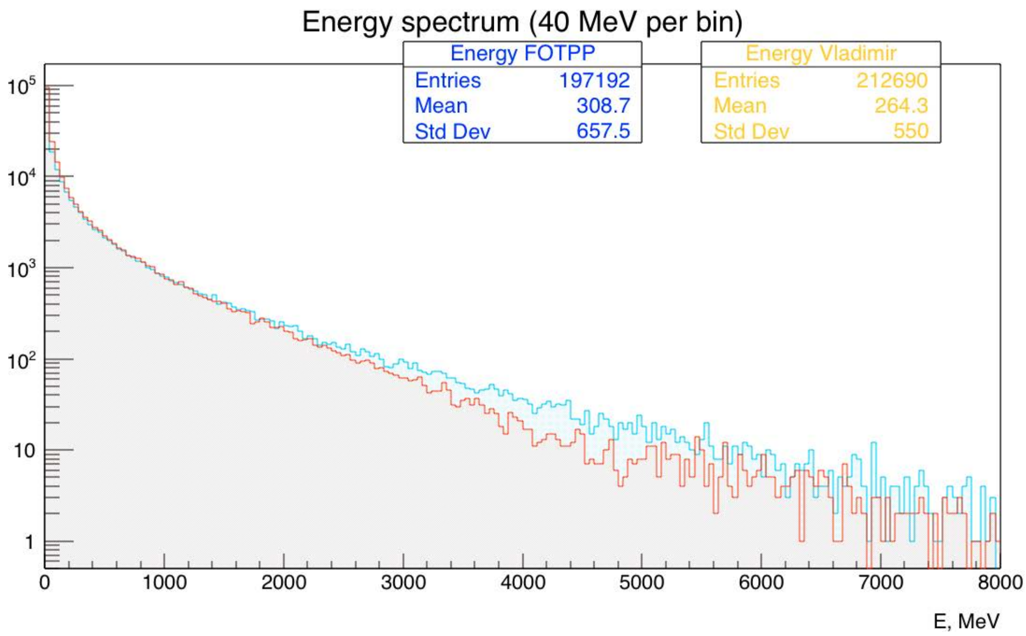


Fig. 2.1.2 – Energy spectrum of the photons (FOTPP and Vladimir`s program)

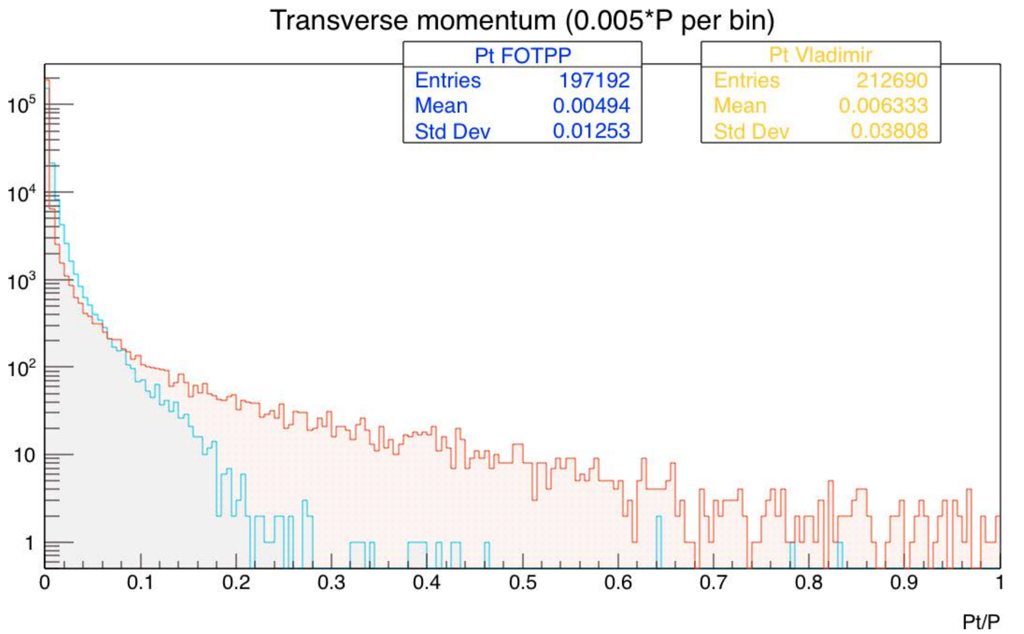


Fig. 2.1.2 – Transverse momentum of the photons (FOTPP and Vladimir`s program)

### 2.1.1 Initial parameters

And how we can see, results were mediocre, that's why was decided to check the initial simulation parameters.

- *PHOMIN* - minimum energy of the photons (GeV);
- *ETMAX* and *VTMAX* - cut-off of ejection (GeV and rad);
- *ZEXIT* – crystal thickness (angstrom);
- *POIMIN* - crystal mode ( = 1 – normal, < 1 – thin crystal);
- *FRECUMA* - frequency of shots (1/angstrom).

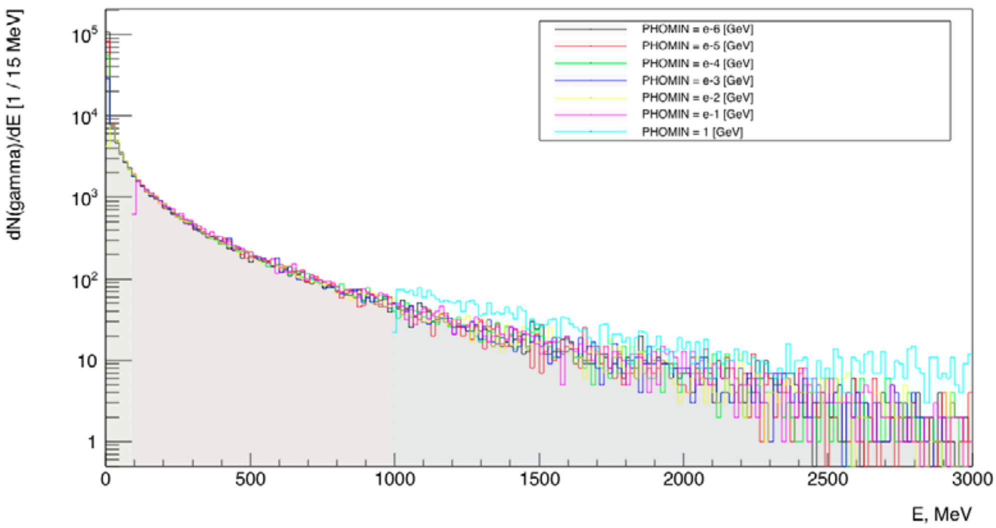


Fig. 2.1.1.1 – Energy spectrum of the photons in dependence on PHOMIN

| PHOMIN, GeV | Number of $\gamma$ | E mean, MeV | $\chi$ mean, % |
|---|---|---|---|
| $10^{-6}$ | 149945 | 62.62 | 1.968 |
| $10^{-5}$ | 125062 | 75.36 | 1.942 |
| $10^{-4}$ | 98081 | 96.17 | 1.892 |
| $10^{-3}$ | 71757 | 130.6 | 1.886 |
| $10^{-2}$ | 47620 | 197.4 | 1.784 |
| $10^{-1}$ | 21991 | 402.8 | 1.717 |
| 1 | 2988 | 1587 | 1.698 |

Work on optimizing the simulation parameters is not finished yet.

### 2.1.2 Generator

For all of the simulations by using the FOTPP have been needed a files "with initial electron beam" which were created by using Geant4. (Project "Generator")

## 2.2 Amorphous converter

A hybrid source scheme (see Fig. 2.1) is composed of a crystal target and an amorphous converter. Our simulation was done for 10 GeV e- beam passed through the crystal. In the role of the converter have been used two kinds of targets: a compact and granular.

Compact converter is an 8 mm thickness and 15 mm radius tungsten cylinder. In its turn, granular converter is 6 layers (10x10 and 9x9) of tungsten sphere with 1.1 mm radius.

The main parameter which was checked is the energy deposition and a PEDD (Peak Energy Deposited Density).

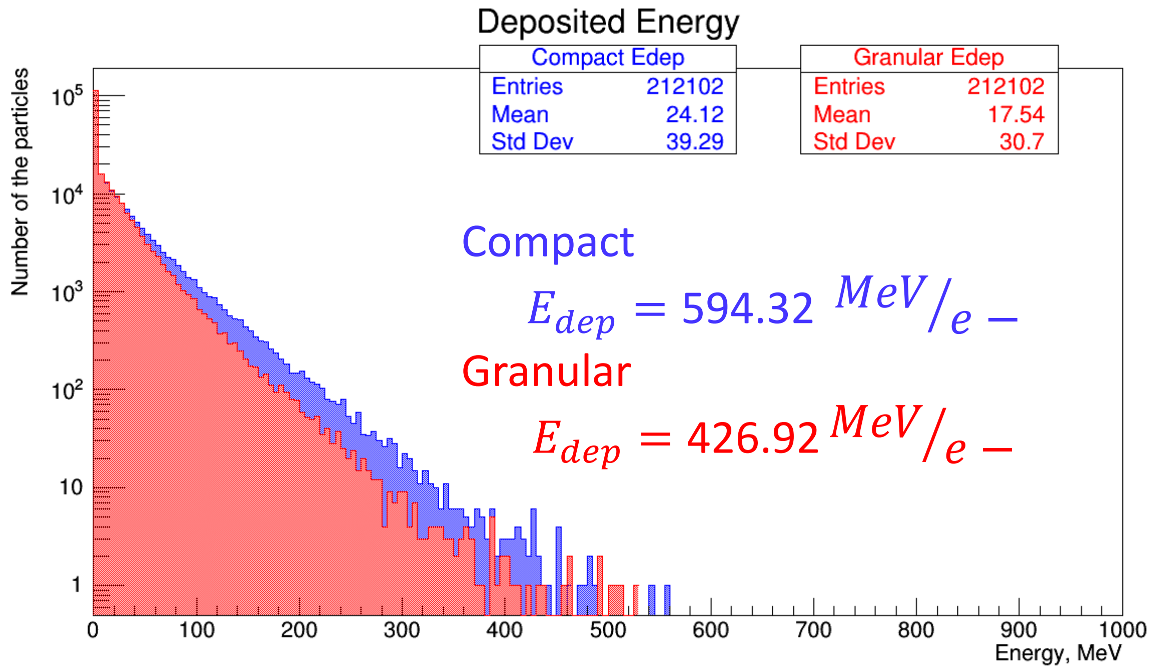


Fig. 2.2.1 – Deposited energy in target volume ((Compact) and (Granular))

For compact converter we have:

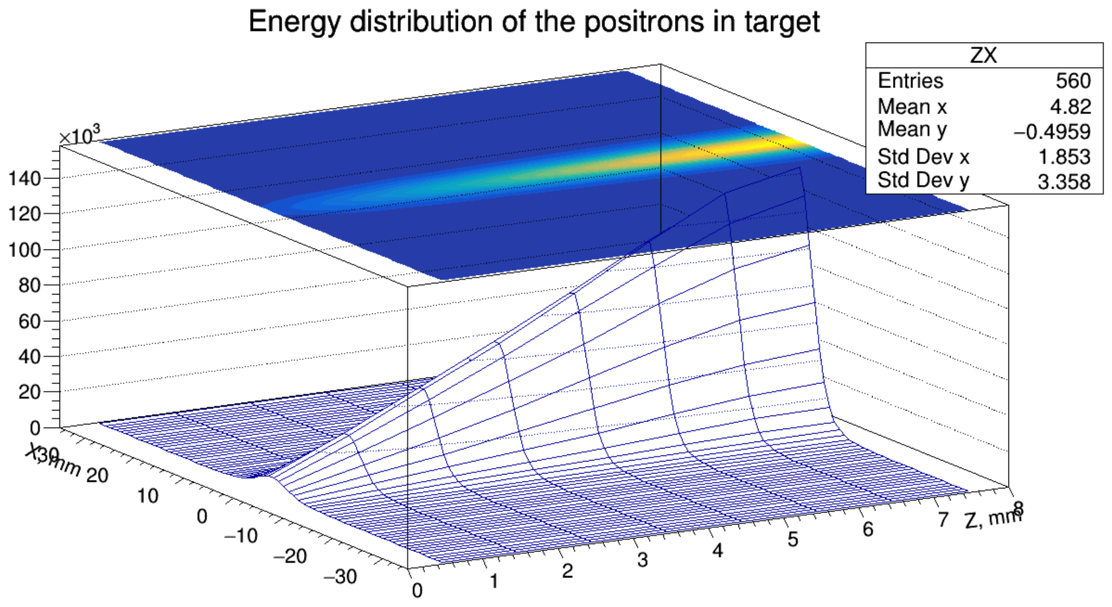


Fig. 2.2.2 – XZ projection of deposited energy distribution in target
(Fig. 1.3.7 binning was used)

Maximum of the deposited energy at the end of our cylindrical target (in the small central cylinder).

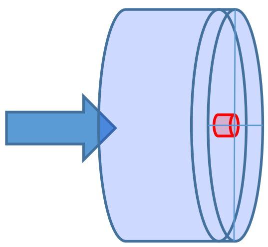

$$PEDD = E_{dep} / V \cdot N_{e-}$$

$$V = H \cdot S = H \cdot \pi \cdot R^2 = {}^{4}/_{3}\, \pi \cdot R^3$$

$$V = 0.00557528\ cm^3$$

**In maximum (last central cylinder):**

$$PEDD = 2.191\ GeV/cm^3 \cdot e-$$

$$Total = 12.214\ MeV/e-$$

For granular:

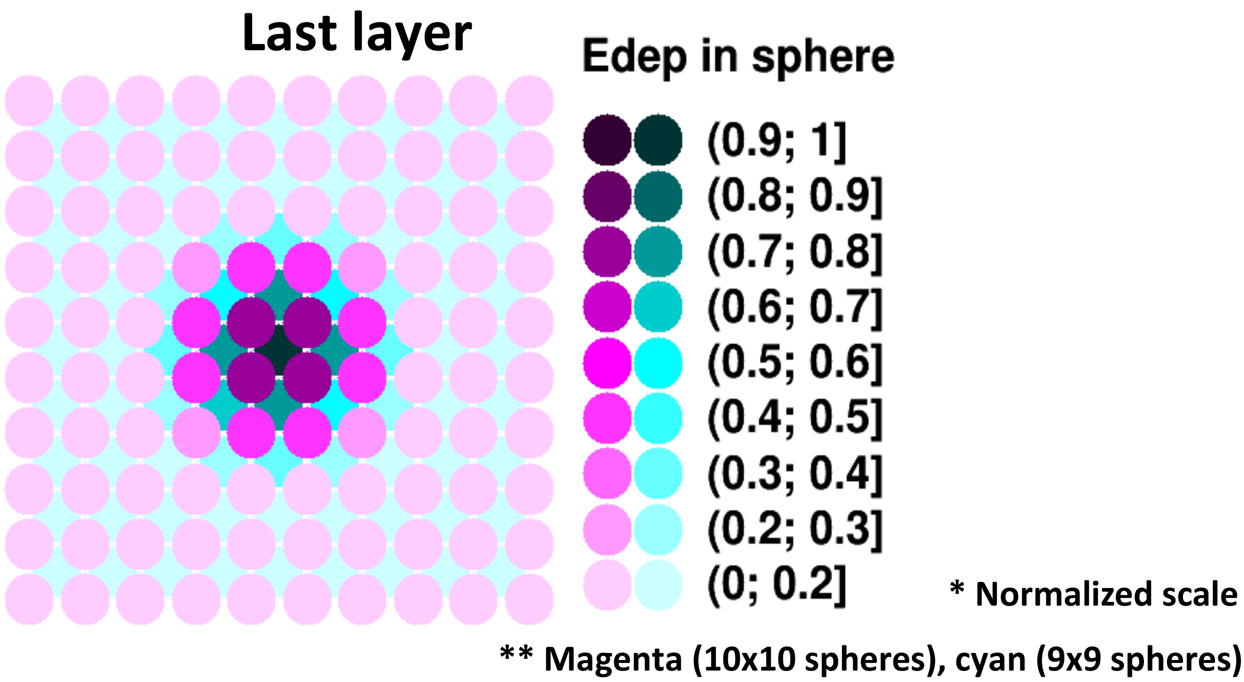


Fig. 2.2.3 – Deposited energy in last two layer of the target

According to Fig. 2.2.3, maximum of the deposited energy is in the last central sphere as we expected.

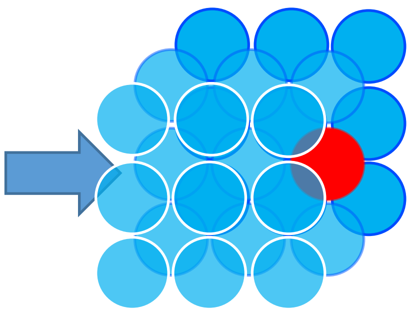

$$PEDD = {E_{dep}}/{V \cdot N_{e-}}$$

$$V = {4}/{3}\,\pi \cdot R^3 = 0.00557528\ cm^3$$

**In maximum (last central sphere):**

$$PEDD = 1.931\ {GeV}/{cm^3} \cdot e-$$

$$Total = 10.765\ MeV/e-$$

So, how we can see (and, of course, as we expected), PEDD and Edep smaller in granular target than in compact.

| • **Before target** | INITIAL γ BEAM | BEFORE COMPACT | BEFORE GRANULAR |
|---|---|---|---|
| Number of the γ per e- | 26.51 | 24.64 | 24.34 |
| $E_{\mathrm{mean}}$, MeV | 312.9 | 333.2 | 335.9 |
| $\sigma_x, \sigma_y$, mm | 2.479, 2.471 | 3.294, 3.276 | 3.148, 3.135 |

| • **After target** | AFTER COMPACT | AFTER GRANULAR |
|---|---|---|
| Number of the e+ per e- | 16.10 | 14.19 |
| $E_{\mathrm{mean}}$, MeV | 85.66 | 99.47 |
| $\sigma_x, \sigma_y$, mm | 3.207, 3.188 | 3.283, 3.272 |
| $E_{\mathrm{dep}(mean)}$, MeV/e- | 594.32 | 426.92 |
| $P_{t(mean)}$, MeV/c | 8.173 | 8.031 |

| • **After magnet (50 cm)** | AFTER COMPACT | AFTER GRANULAR |
|---|---|---|
| Number of the e+ per e- | 5.56 | 5.24 |
| $E_{\mathrm{mean}}$, MeV | 145.9 | 166.9 |
| $\sigma_x, \sigma_y$, mm | 9.054, 9.048 | 9.143, 9.146 |
| $P_{t(mean)}$, MeV/c | 3.998 | 4.104 |

## 2.3 Electric field

The final stage of my internship is the implementation of the electric field (acceleration of the positrons) to my previous simulation with a granular converter.

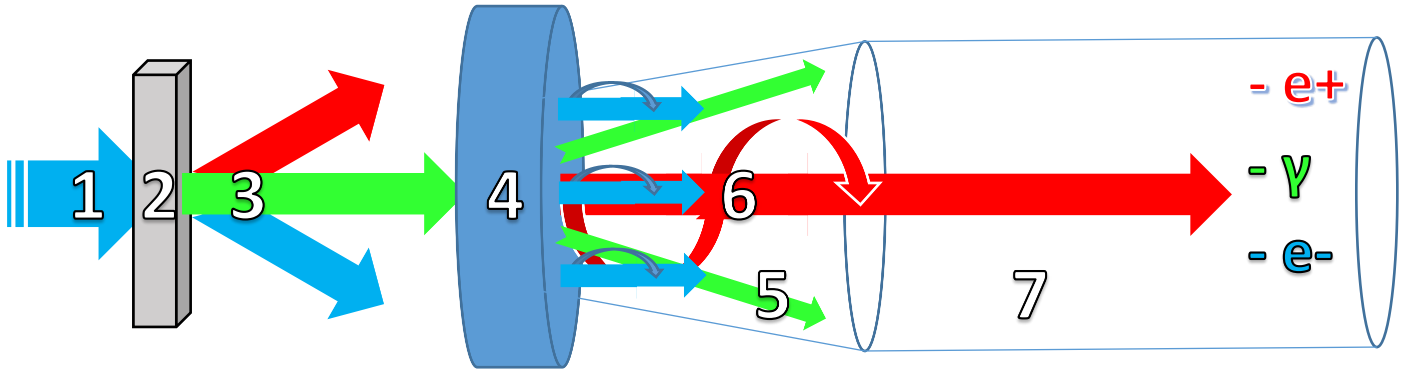


1 Initial e- beam;
2 Crystal;
3 Initial γ beam;
4 Target;
5 AMD;
6 Outcome e+ beam;
7 Accelerator.

Fig. 2.3.1 – Principal scheme of the modern hybrid source simulation

The accelerating section is the 1 m cylindrical volume with the same 2 mm copper skin such as AMD have. In this accelerating section, we have a 15 MV/m electric field along the Z axis.

### Some results of the simulation

| • **Before target** | **INITIAL γ BEAM** | **BEFORE TARGET** |
|---|---|---|
| **Number of the γ per e-** | **26.51** | **24.34** |
| $E_{mean}$, **MeV** | **312.9** | **335.9** |
| $\sigma_x, \sigma_y$, **mm** | **2.479, 2.471** | **3.148, 3.135** |

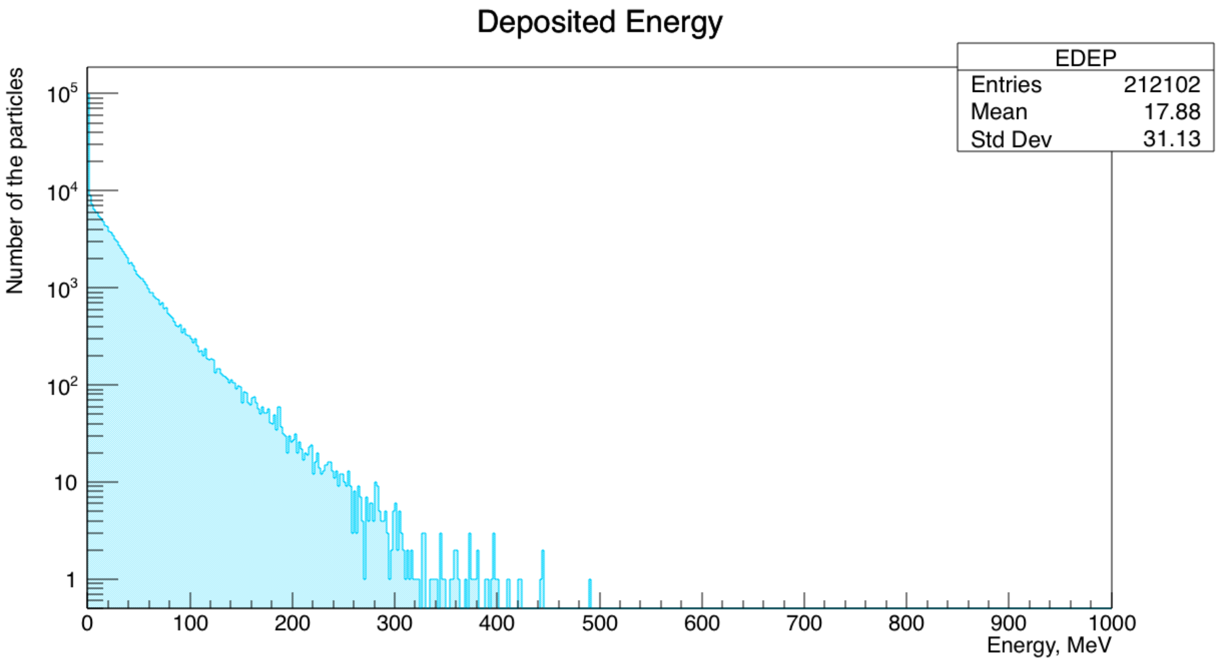


Fig. 2.3.2 – Deposited energy in the granular target

$(E_{dep} = 435.19\, {}^{MeV}/_{e\,-})$

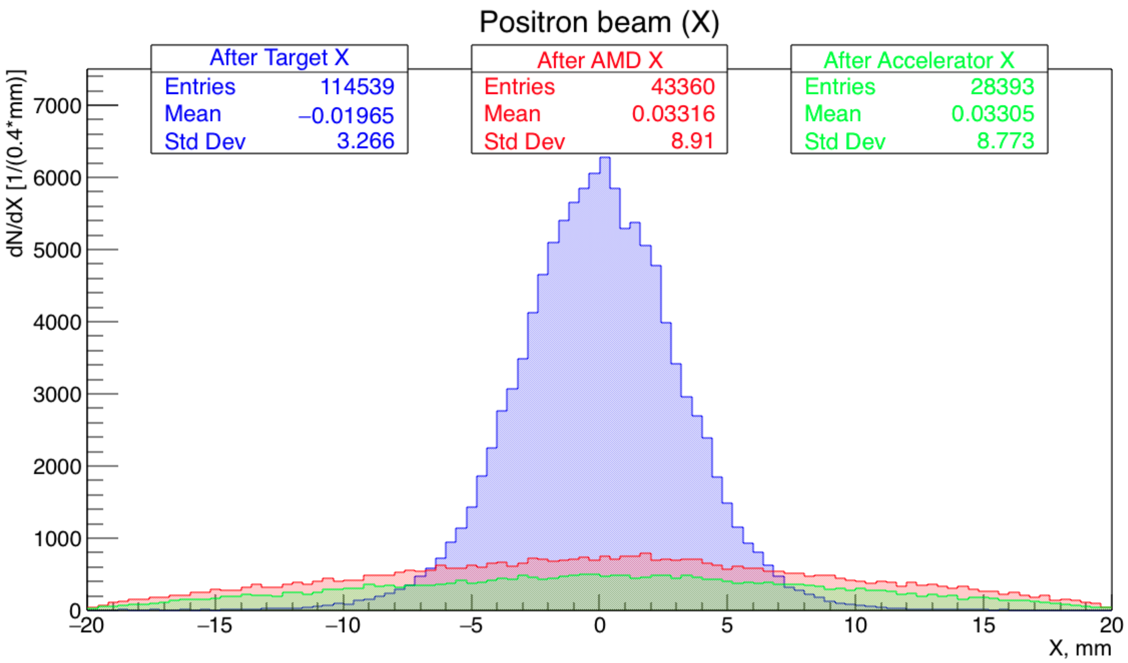


Fig. 2.3.3 – X projection of spatial distribution of the e+ beam

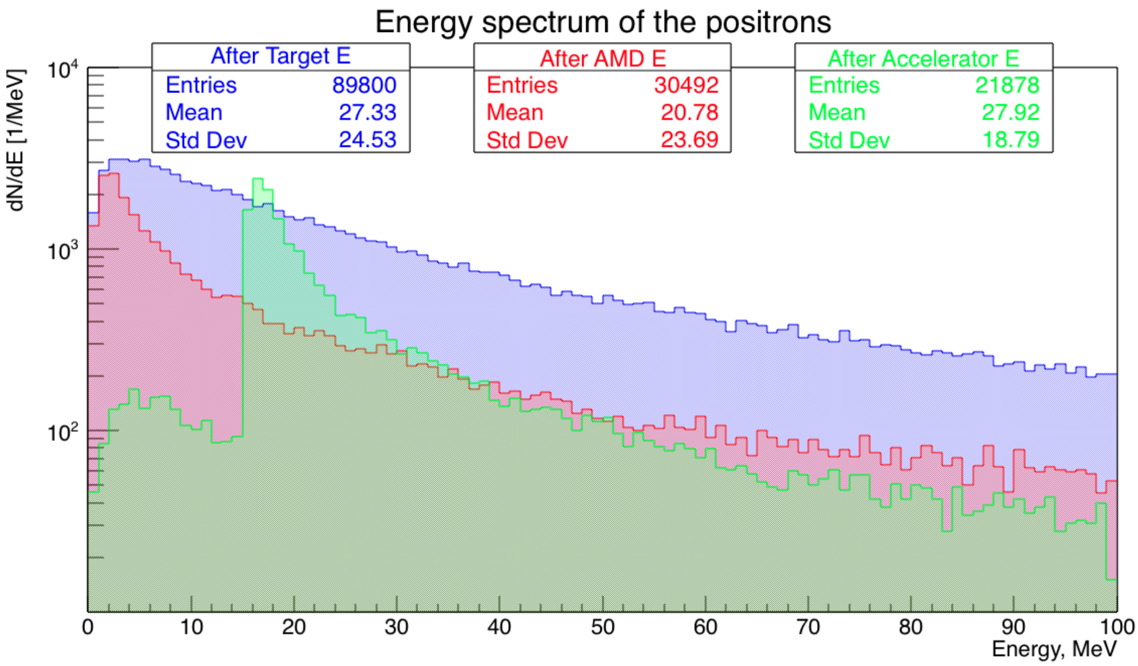


Fig. 2.3.4 – Energy spectrum of the e+ beam [0-100 MeV]

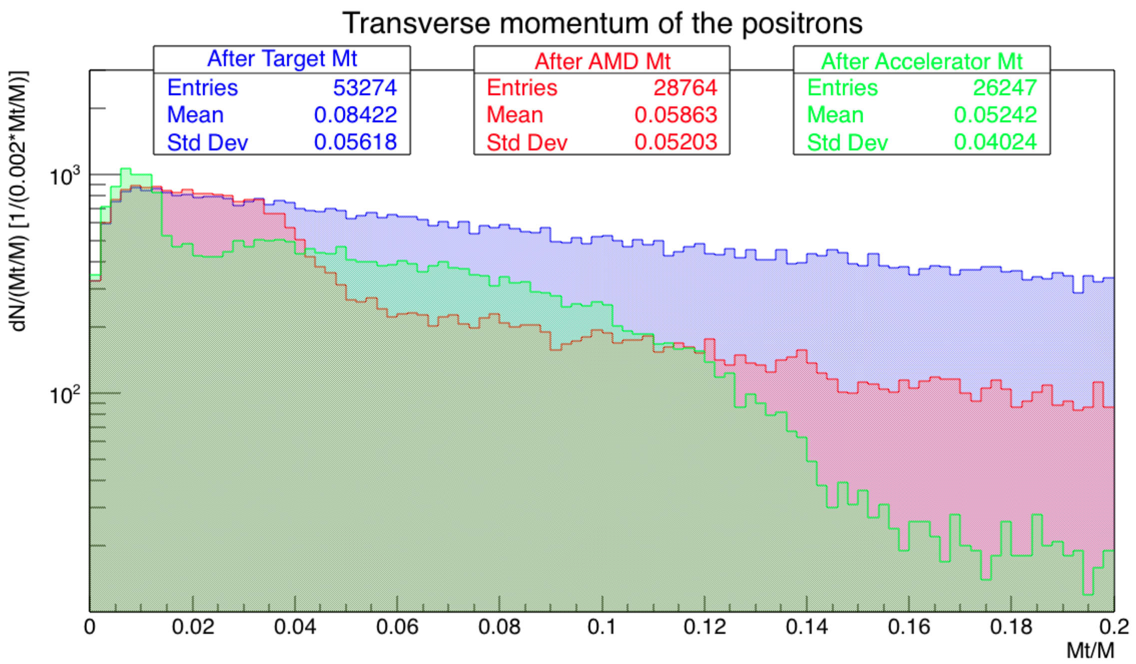


Fig. 2.3.5 – Transverse momentum of the e+ beam [0-0.2 Pt/P]

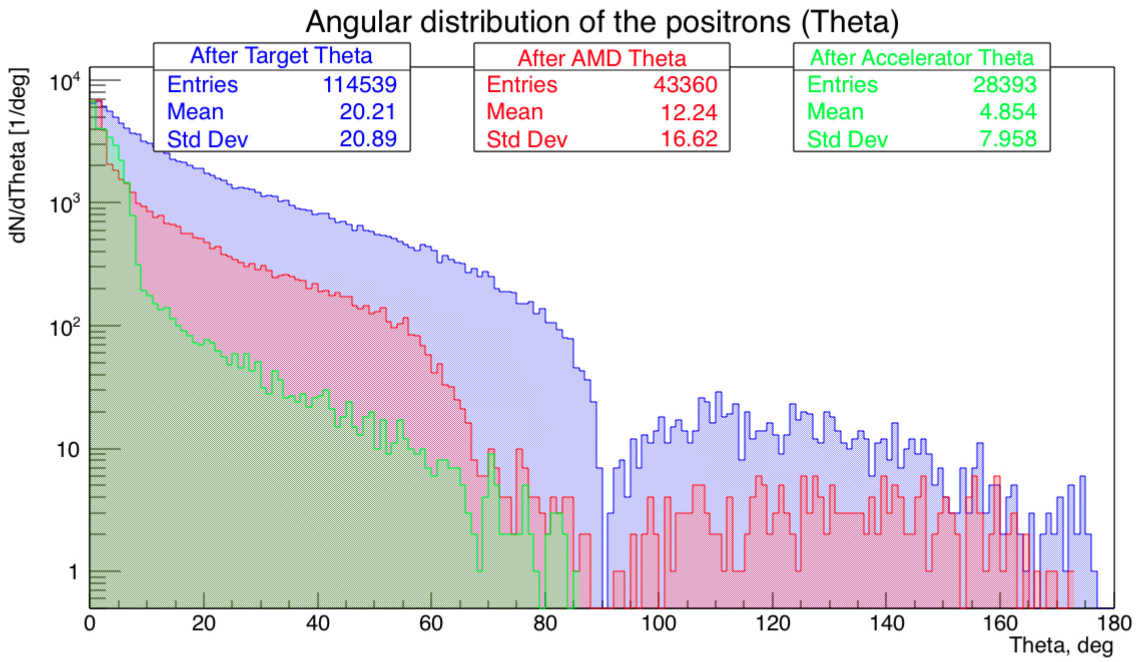


Fig. 2.3.6 – Angular distribution of the e+ beam (Theta)

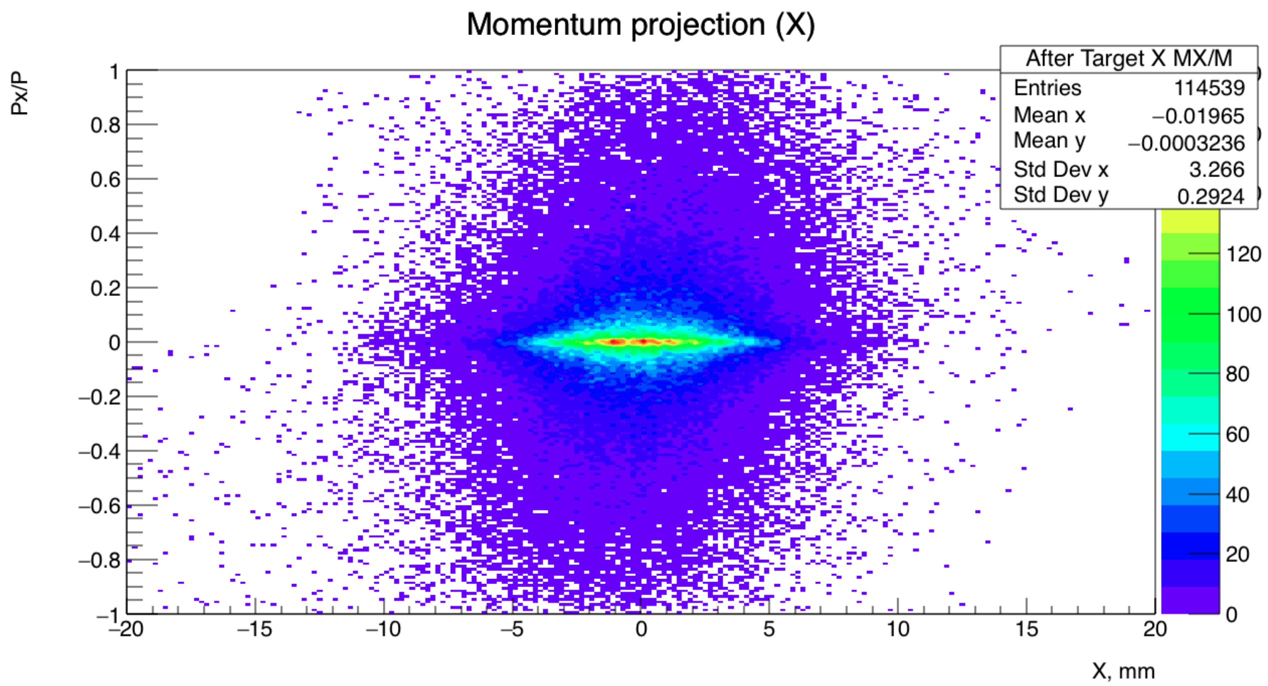


Fig. 2.3.7 – Transverse momentum versus X coordinate of the e+ after target

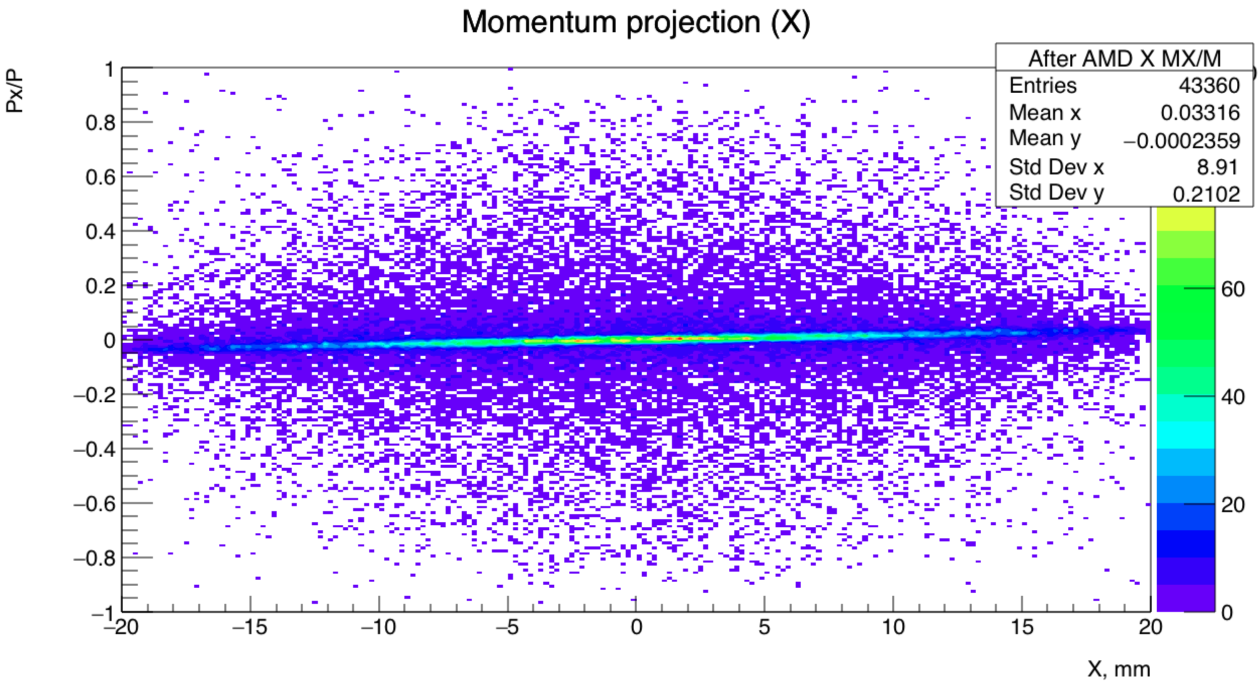

Fig. 2.3.8 – Transverse momentum versus X coordinate of the e+ after AMD

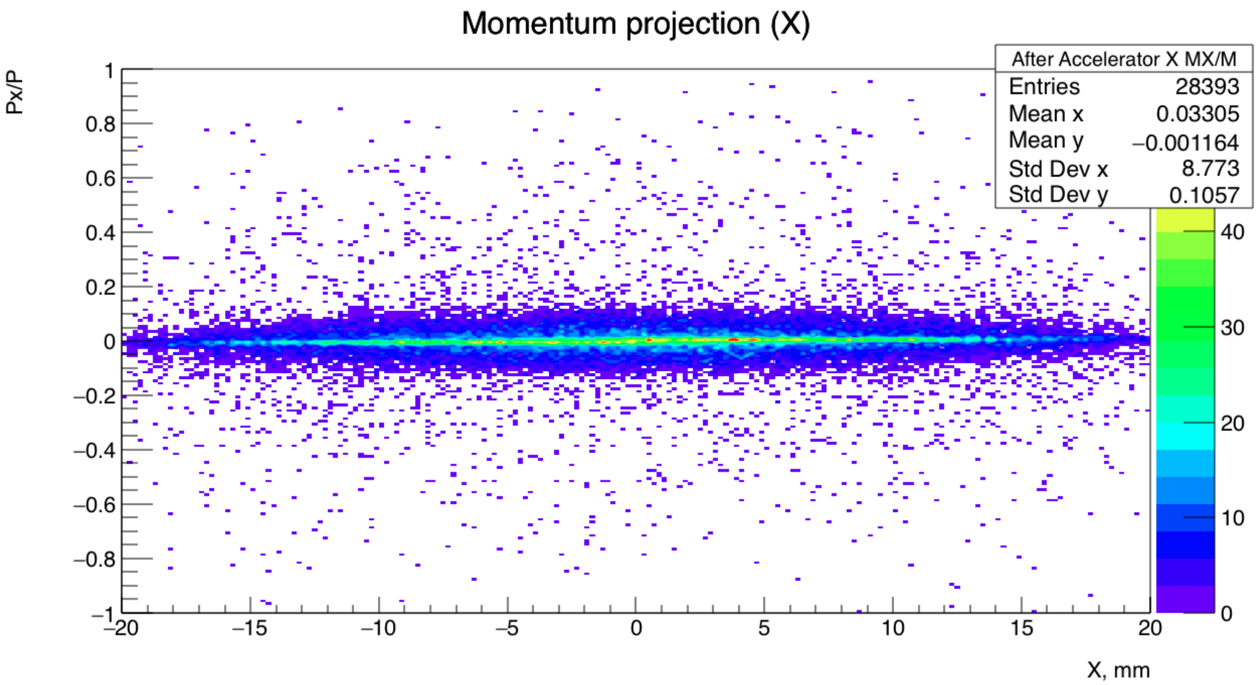

Fig. 2.3.9 – Transverse momentum versus X coordinate of the e+ after electric field